European Journal of Pharmaceutics and Biopharmaceutics 77 (2011) 225–232

Contents lists available at ScienceDirect

European Journal of Pharmaceutics and Biopharmaceutics

journal homepage: www.elsevier.com/locate/ejpb

Research paper

Thermosensitive hydrogels for nasal drug delivery: The formulation and characterisation of systems based on *N*-trimethyl chitosan chloride

H. Nazar [a], D.G. Fatouros [a], S.M. van der Merwe [a], N. Bouropoulos [b,c], G. Avgouropoulos [b,c], J. Tsibouklis [a], M. Roldo [a,*]

[a] School of Pharmacy and Biomedical Sciences, University of Portsmouth, Portsmouth, UK
[b] Department of Materials Science, University of Patras, Patras, Greece
[c] Foundation for Research and Technology – Hellas (FORTH), Institute of Chemical Engineering and High Temperature Chemical Processes (ICE-HT), Patras, Greece

ARTICLE INFO

Article history:
Received 28 March 2010
Accepted in revised form 29 November 2010
Available online 3 December 2010

Keywords:
Chitosan
N-trimethyl chitosan chloride
Thermosensitive
Mucoadhesion
Hydrogel
Nasal drug delivery

ABSTRACT

Towards the development of a thermosensitive drug-delivery vehicle for nasal delivery, a systematic series of *N*-trimethyl chitosan chloride polymers, synthesised from chitosans of three different average molecular weights, have been co-formulated into a hydrogel with poly(ethylene glycol) and glycerophosphate. Rheological evaluations have shown that hydrogels derived from *N*-trimethyl chitosan with a low degree of quaternisation and high or medium average molecular weight exhibit relatively short sol–gel transition times at physiologically relevant temperatures. Also, the same hydrogels display good water-holding capacity and strong mucoadhesive potential, and their mixtures with mucus exhibit rheological synergy. An aqueous hydrogel formulation, derived from *N*-trimethyl chitosan of medium average molecular weight and low degree of quaternisation, appears particularly promising in that it exhibits most favourable rheological and mucoadhesive behaviour and a sol–gel transition that occurs at 32.5 °C within 7 min.

1. Introduction

Since patient acceptability of nasal administration is high [1], and owing to the avoidance of the first-pass effect, the nasal mucosal membrane presents a potentially useful site for the delivery of proteins and peptides [2–6]. However, there are drug-delivery challenges that need to be overcome if intranasal drug delivery is to become the method of choice for the delivery of therapeutic agents, namely: mucosal membranes pose a substantial barrier to the absorption of macromolecules [7]; proteolytic enzymes in nasal secretions impact upon the bioavailability of proteins and peptides [1]; and nasal residence, as determined by mucus turnover time, is limited to approximately 15–20 min [1,8]. Drug-delivery strategies that have been explored in efforts to overcome these challenges are as diverse as the modification of the peptide structure [9], the inhibition of the ciliary beat frequency [1], the employment of permeation or absorption enhancers, and the utilisation of mucoadhesive polymers [10].

Research efforts into the employment of mucoadhesive viscoelastic hydrogels in nasal drug delivery are rationalised in terms of their potential for prolonging the residence time of the active on the mucosal surface. Such systems lend themselves to administration as sprays or drops and may be designed such that they undergo a sol–gel transition at the temperature of the site of deposition (32–35 °C, see ESI) [11,12], with the implication that the increased viscosity and rheological synergy of the resulting mucus/mucoadhesive system effects prolonged residence at the site of action [13–17].

Amongst the mucoadhesive viscoelastic hydrogels studied to date, those structured around chitosan – a biocompatible and biodegradable natural polysaccharide – have shown particular promise since they facilitate the paracellular transport of large molecules across the mucosal surface by opening tight junctions [18–22]. In particular, the thermosensitive chitosan/glycerophosphate gels, developed by Chenite et al. [23], were shown to be suitable for the delivery of sensitive biological materials such as proteins and gene-based therapeutics. However, despite promising results, chitosan presents limitations in that it is only soluble and active in acidic environments, when in its protonated form [24]. For this reason, and due to the fact that the chitosan-based thermosensitive gels so far developed undergo only a slow sol–gel transition at physiological pH [25], chitosan has been substituted by its positively charged derivative *N*-trimethyl chitosan chloride (TMC) [26]; this retains the key qualities of the parent polymer but presents improved solubility profile, enhanced mucoadhesive

* Corresponding author. School of Pharmacy and Biomedical Sciences, University of Portsmouth, Portsmouth, Hampshire PO1 2DT, UK. Tel.: +44 2392843586; fax: +44 2392843565.
E-mail address: marta.roldo@port.ac.uk (M. Roldo).

0939-6411/$ - see front matter © 2010 Elsevier B.V. All rights reserved.
doi:10.1016/j.ejpb.2010.11.022

properties and a significant absorption enhancing effect over a wide pH range [27] as well as enhancing the properties of the thermosensitive formulations [14,23,28]. TMC/GP hydrogels have been previously studied for parenteral drug delivery [25,29]; however, there are scarce reports on their use for intranasal administration. Therefore, the current work aims at investigating this specific application, studying the effect of molecular weight (MW) and degree of quaternisation (DQ) of TMC, as well as hydrogel composition on the thermosensitivity and rheological behaviour of nasal formulations. The objective is to optimise a system able to undergo a sol–gel transition in the temperature range 32–35 °C, thereby allowing a stable liquid state to be maintained at storage temperature and prior to usage, easing administration via nasal spray or drops. This system should gel at 32–35 °C, representative of the nasal environment [12], and provide a synergic effect in contact with the nasal mucus that can guarantee prolonged residence time and show the required rheological characteristics. These have been identified to be specific apparent viscosity (350 mPa s) and viscoelasticity (200 Pa) values that significantly reduce the mucociliary transport rate (MTR) [30].

2. Materials and methods

2.1. Materials

Chitosans (low viscosity, 150 kDa, degree of deacetylation (DD) 95–98%; medium viscosity, 400 kDa, DD 84–89%; and high viscosity, 600 kDa, DD 75–85%), poly(ethylene) glycol 4000 (PEG) and poly(acrylic acid) (PAA) were obtained from Fluka, UK. Glycerophosphate (GP; equimolar mixture of α and β isomers), tristearin (TRIS) and porcine-stomach mucin were purchased from Sigma–Aldrich Inc., UK. Methyl iodide and 1-methyl-2-pyrrolidinone were sourced from Acros Organics, Belgium. All other chemicals were obtained from Fisher Scientific, UK, and used as received.

2.2. Synthesis and characterisation of N-trimethyl chitosan chloride

TMC was synthesised *via* the reductive methylation of chitosan of three different average molecular weights (low, L; medium, M and high, H) according to the method described by Sieval et al. [26] (see ESI for detailed method). Different degrees of quaternisation were obtained by employing a one- and a two-step synthesis method (e.g. L1 or L2) as described by Hamman and Kotze [31]. The degree of quaternisation was calculated from corresponding ^{1}H NMR spectra (D_2O; 80 °C; Jeol 400 MHz spectrometer, Bruker, Japan) using Eq. (1) [32]:

$$DQ\% = \frac{(\int 3.4)}{(\int 4.7{-}5.4)} \times \frac{1}{9} \times 100 \quad (1)$$

where DQ is the degree of quaternisation, and $\int$3.4 and $\int$4.7–5.4 are the respective integrals of the trimethyl amino group absorption (3.4 ppm) and of the collective ^{1}H resonances in the range 4.7–5.4 ppm [26]. Infrared spectra were recorded using a Varian 640-IR FTIR (Varian Inc., Palo Alto, USA; 400–4000 cm^{-1}, absorbance mode, 4 cm^{-1} resolution, 32 scans). Thermogravimetric analysis (TGA) was performed using a TGA-Q50 (TA Instruments, New Castle DE, USA; N_2 atmosphere, 10–600 °C, 10 °C min^{-1}). The crystalline order of dry TMC polymers was examined using an X-ray diffractometer (Bruker D8, Karlsruhe, Germany; Ni-filtered Cu Ka_1, wavelength (λ) = 0.154059 nm at 40 kV, 40 mA, scan speed = 1 deg min^{-1}, 2θ range 2–50°). Fourier Transform Raman (FT-Raman) spectra were recorded using a Bruker EQUINOX 55 spectrometer (Karlsruhe, Germany) equipped with a (D) FRA-106/S attachment: Raman excitation was by means of a A R510 diode pumped Nd:YAG laser operating at 1064 nm (with a maximum output power of 500 mW); optical filtering reduced the Rayleigh elastic scattering and, in combination with a CaF_2 beamsplitter and a high sensitivity liquid N_2-cooled Ge-detector, allowed the Raman intensities to be recorded over the range 50–3300 cm^{-1} in the Stokes side.

2.3. Formulation and characterisation of hydrogels

For each synthesised TMC polymer, 4 TMC solutions with a concentration of 4.5% w/v and a total volume of 4 mL were prepared in deionised water. To the TMC solutions, PEG 4000 (270 mg) was added with stirring until a clear solution was obtained. In parallel, a series of aqueous GP solutions of specified concentrations (6.25, 12.5, 25 and 50% w/v) were also prepared. All solutions were placed in an ice bath for 10 min. Hydrogels were prepared by the dropwise addition (under stirring) of 1 mL aliquots of the cold GP solution to each of the cold TMC/PEG solutions, and gel compositions are given in Table 1.

2.3.1. Visual determination of sol–gel transition time

The sol–gel transition time was determined by visual inspection, using the inversion method [33]: TMC/PEG/GP solutions (5 mL) were incubated in a water bath at 35 °C or left at room temperature for the duration of the test, and at 30 s intervals, the vials were inverted to assess the flowage of the sample; the sol and gel phases were respectively characterised by the sample exhibiting liquid-like flow or becoming immobile. All experiments were carried out in quadruplicate.

2.3.2. Rheological investigations

Rheological analysis (cone and plate geometry; cone dimensions 2° and 60 mm diameter) was performed using an AR2000 controlled-stress rheometer (TA Instruments, Leatherhead, Surrey, UK) interfaced to TA Rheology Data Analysis software (V.5.1.42, TA Instruments, Leatherhead, Surrey, UK). Aliquots of test samples were loaded onto the rheometer platform and allowed to equilibrate (5 min) at the temperature of the experiment. Strain sweep measurements at 1 Hz (n = 1) allowed the determination of the linear viscoelastic region (LVR); where appropriate, further rheological investigations were performed within this region.

2.3.3. Assessment of in vitro sol–gel transition time and temperature

To assess the physiological relevance of the sol–gel transition time of TMC hydrogels, rheological evaluation tests were performed at 15 °C and at 35 °C; temperatures that respectively correspond to that of cool storage and that of the surface of the nasal mucosa [12]. For formulation M1-2.5GP, the experiment was also carried out at 25, 27, 29, 31 and 33 °C, to study the effect of temperature on gelation time. A multiwave frequency test allowed the determination of the frequency-independent gelation time from the intersecting curves tan δ *versus* time. A time sweep (1 °C min^{-1}) was performed over the 10–40 °C temperature range, at a fixed frequency (0.01 Hz) and a fixed amplitude of applied stress (0.02 Pa). The gelation temperature was determined by monitoring the variations in the elastic (G') and viscous (G'') moduli: gelation temperature was identified by the transition from a prevalently viscous state ($G'' > G'$) to one that is prevalently elastic ($G' > G''$). All experiments were carried out in quadruplicate.

Table 1
The composition of the TMC hydrogel formulations.

Component	Final concentration (% w/v)
TMC (L1, L2, M1, M2, H1, H2)	3.6
PEG 4000	5.8
GP	1.25, 2.5, 5, 10

2.4. Preparation of mucus/hydrogel systems

Since the capability of hydrogels to form true blends with mucus is a property of some importance to the *in vivo* mucoadhesion behaviour of the system and also its influence upon the mucociliary transport rate (MTR), hydrogel/mucus mixtures for rheological and other investigations were prepared by mixing the hydrogel formulations with simulated nasal electrolyte solution (SNES: 7.45 mg mL^{-1} NaCl; 1.29 mg mL^{-1} KCl and 0.32 mg mL^{-1} $CaCl_2{\cdot}2H_2O$; adjusted to pH 5.5 with 1 M aqueous HCl and mixed with 1 mg mL^{-1} aqueous mucin in the 5:1 (w/w) ratio). Controls were provided by similar, 5:1 (w/w), mixtures of hydrogel and water and also of water and mucin.

2.4.1. Viscosity, viscoelasticity and rheological synergy

Frequency sweeps (10–0.01 Hz, 20 readings) on hydrogel/mucus mixtures allowed the determination of the complex modulus, G^*; evaluation studies confirmed there was no significant difference between the 20 readings of G^*. Measurements of G' and G'' were also averaged over 20 readings. The synergistic effect of hydrogel and mucin mixtures was evaluated using Eq. (2) [34]:

$$\text{Relative } G' = \frac{G'_{mix} - (G'_{Hyd} + G'_{Muc})}{G'_{Hyd} + G'_{Muc}} \quad (2)$$

where $G'_{mix}, G'_{Hyd}, G'_{Muc}$ represent the respective elastic moduli of hydrogel–mucin mixtures, hydrogel and mucin; relative G'' was calculated similarly.

The apparent viscosities (η) of the hydrogel and of the hydrogel–mucin samples were monitored for 1 min under constant shear rate (100 s^{-1}); experiments were repeated four times, and measurements are reported as the average of those taken during the final 30 s of each measurement period. Oscillatory measurements (40–0.01 Hz; constant applied stress, within the LVR) allowed the investigation of the effects of frequency on the dynamic moduli, G' and G'', and provided the means for the assessment of rheologically synergistic effects.

2.5. Water-holding capacity of hydrogel formulations

The capacity of the hydrogels to hold absorbed water was evaluated as a function of molecular weight and the degree of quaternisation. Discs were cut (diameter 15 mm, cross-sectional thickness 5 mm) from freeze-dried hydrogel and dried at 60 °C for 24 h. These were placed into dissolution baskets, which were then immersed into pH 5.5 SNES-mucin (20 °C) for specified periods of time. The baskets were lifted out of the solution and each weighed following the repetitive wiping of excess surface liquid (filter paper) until three consecutive readings gave identical mass readings. The water-holding capacity (WHC) was calculated from:

$$\text{WHC} = \frac{M_{Max} - M_0}{M_0} \quad (3)$$

where M_{Max} is the maximum mass of the hydrated gel, and M_0 is the mass of the dry gel at time 0.

2.6. Mucoadhesive behaviour

A TA-XT2 Texture Analyser (Stable Micro Systems, Surrey, UK) in adhesion mode allowed the determination of the total work required to detach the lyophilised hydrogels from isolated rat intestinal mucosal tissue [35]. Positive and negative controls were provided by samples of poly(acrylic acid) and tristearin, respectively. Test materials or controls were attached to the lower tip of the texture-profile-analyser probe using double-sided adhesive tape. The substrate was Wistar rat intestinal mucosa that had been isolated surgically and kept in mucin solution (pH 5.5). For force measurements, the tip was lowered onto the surface of the mucosa, a force of 0.02 N was applied for 2 min, to ensure intimate contact between the mucosal surface and the hydrogel sample, and the probe was raised at a constant speed of 5.00 mm s^{-1} to a return distance of 300 mm. The total work-of-adhesion (TWA) was calculated from the area under the force *versus* distance curve and reported as the average of four measurements. Data collection and manipulation was by means of an interfaced XTRA Dimension software package.

2.7. Statistical analysis

The statistical significance of the differences between rheological and mucoadhesive parameters of the range of TMC/PEG/GP hydrogel formulations was tested by one-way analysis of variance (ANOVA) and further by the multiple comparison Tukey–Kramer test. Differences were considered to be significant if $p < 0.05$.

2.8. Physicochemical characterisation of hydrogels

The porosity and surface area of the lyophylised hydrogels were determined using the Brunauer–Emmett–Teller (BET) method. The specific surface area (S_{BET}), the pore volume (V_P) and the pore size distribution of the samples were determined (Quantachrome Autosorb-1 instrument; Boynton Beach, FL, USA) from the adsorption/desorption isotherms of nitrogen at −196 °C. The surface area was obtained following the BET procedure with six relative pressures of nitrogen in the range 0.05–0.3p_0. Pore size distribution was estimated using the BJH (Barrett, Joyner and Halenda) method. Total pore volume was determined (out-gassed samples; room temperature, 10 h, vacuum) at $P/P_0 = 0.995$. The surface morphology and internal structure of hydrogels were visualised by scanning electron microscopy (SEM; JEOL SEM JSM-6060LV, JEOL Ltd., Japan; working distance 12–14 mm at 10 kV, spotsize 35 μm): flat surface cross-sections of dried samples were prepared using a sharp blade and imaged under vacuum after 3 min of palladium/gold sputtering; displayed images are at 3000× magnification.

3. Results and discussion

3.1. TMC synthesis and characterisation

Consequent to the quaternisation reaction, vibrational spectra exhibited the features that differentiate TMC polymers from their precursor chitosans. Indicative of the destruction of residual amidic linkages during the quaternisation reaction, Raman spectra (Fig. 1) showed that the intense CH_3 absorption of acetamide groups (1380 cm^{-1}), the amidic carbonyl band (1657 cm^{-1}) and the weak amidic N–H stretch (3367 cm^{-1}) all disappeared on quaternisation [36,37]. Infrared spectra (Fig. 1) showed the characteristic band (3300–3500 cm^{-1}) that is consistent with the presence of hydrogen-bonded –NH_2 and –OH functionalities. As expected, the intensity of the amino group bend, at 1597 cm^{-1}, weakened on quaternisation. Indicative of the specificity of the reaction, primary and secondary alcohol absorptions (1102–1082 cm^{-1}) appear little changed following quaternisation [28]. Consistent with the introduction of methyl moieties, the C–H stretching bands (2900–3000 cm^{-1}) and bending deformations (1470–1500 cm^{-1}) appeared to become more intense with increasing degree of quaternisation.

The DQ of the synthesised TMC polymers, as calculated from ^1H NMR experiments [26], is presented in Table 2, along with $T_{50\%}$ values from thermogravimetric investigations. In accord with expectation [38], higher DQ polymers exhibited increased thermal stability relative to their respective congeners; a similar trend of

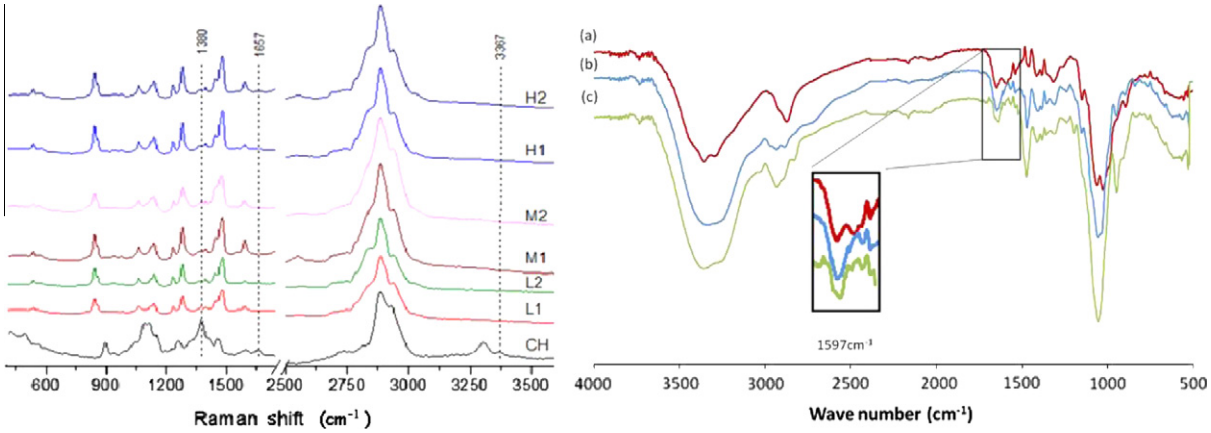

Fig. 1. Left: FT-Raman spectra of chitosan (CH) and TMC polymers (L, low; M, medium and H, high molecular weight; 1, one step synthesis and 2, two-step synthesis). Right: FTIR spectra of (a) low molecular weight chitosan, (b) L1 and (c) L2. (For interpretation of the references to colour in this figure legend, the reader is referred to the web version of this article.)

Table 2
Degree of quaternisation of *N*-trimethyl chitosan chloride polymers synthesised and the temperature required to reduce the respective weight by 50%, $T_{50\%}$, as derived via thermogravimetric analysis. The indexes 1 and 2 refer to the number of steps employed in the synthesis of chitosan.

TMC	Chitosan average molecular weight	DQ (%)	$T_{50\%}$ (°C)
H1	High	25.6	356
H2		53.9	380
M1	Medium	32.8	323
M2		61.3	383
L1	Low	37.0	308
L2		54.6	322

increasing thermal stability was observed with increasing average molecular weight. Consistent with the thermal stability effects, XRD experiments showed the increased crystalline order in TMC samples relative to that of their precursor chitosans, as is indicated by the appearance of pronounced bands at 2ϑ 19.4°, 23.4° and 32.0°, Fig. 2, and the corresponding disappearance of the characteristic chitosan peak at $2\vartheta = 11°$ [39,40].

3.2. Characterisation of hydrogel formulations

3.2.1. Determination of gelation time and temperature

The performance criteria of the nasal-delivery formulations are imposed by the physiological temperature of the nasal cavity (32–35 °C [12]) and by the mucociliary clearance time (half life *ca.* 21 min [41]), which correspondingly specify the temperature range and time limits for the sol–gel transition. The application of the inverted-tube test coupled with rheology investigations allowed the determination of the influence of GP concentration on gelation temperature and gelation time (Fig. 3). The data relative to TMC formulations from low MW chitosan are not shown as they do not exhibit gel-like behaviour over the investigated range of GP concentrations, due to the short polymeric chain which offers limited chances of physical entanglement and hydrophobic interactions. The co-formulation of PEG molecules imparted considerable improvement on the capacity of networks to form gels. Amongst the formulations tested, only hydrogel M1 (2.5% w/v GP) exhibited its sol–gel transition at a physiologically relevant temperature (32.5 ± 0.4 °C; Fig. 3). The gelation time of the same formulation has been determined at 6.3 ± 0.6 min, which is well below the time for mucociliary clearance. The gelation time of this formulation was tested in the 25–35 °C range to ascertain that it would be effective even if the temperature of the nasal cavity was different (Table 3). The formulation underwent sol–gel transition in a time shorter than the half life of the mucociliary clearance at all temperatures above 29 °C. The polyol, GP, provides protective hydration of TMC, maintaining the polymer chains stretched in solution, as the inter- and intra-molecular crosslinking within the system is reduced [14]. Upon raising the temperature to 35 °C, the increased kinetic energy favours the formation of hydrophobic interactions between chains. The addition of PEG

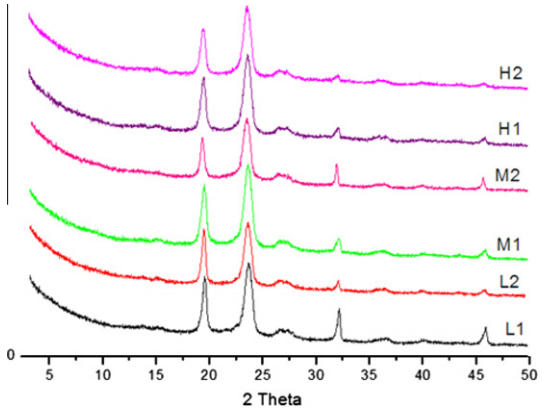

Fig. 2. XRD patterns of TMC polymers. (For interpretation of the references to colour in this figure legend, the reader is referred to the web version of this article.)

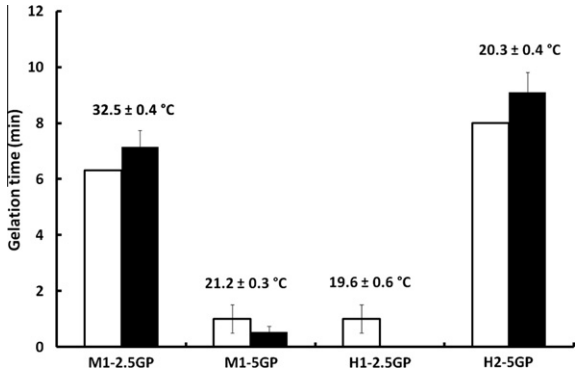

Fig. 3. Rheological (black) and observational (white) gelation time, and rheological gelation temperature of TMC hydrogel formulations (e.g. M1-2.5GP, hydrogel formulated with medium molecular weight TMC, synthesised by one-step procedure and containing 2.5% GP). Results are given as mean ± SD ($n = 4$).

Table 3
Effect of temperature on the gelation time of M1-2.5GP formulation.

Temperature (°C)	Gelation time (min)
29	49.6 ± 3.4
31	16.5 ± 1.9
33	9.3 ± 1.6
35	6.3 ± 0.6

allows the formation of an even more extensive gel network by providing extra sites for hydrogen bonding [14]. Gelation was accompanied by a significant change in viscoelasticity, G^* (Fig. 4a). Apparent viscosity increased with increasing temperature; this increase was not statistically significant for formulation H2 (5% w/v GP) (Fig. 4b). The effect of temperature was most pronounced for formulation M1 (2.5% w/v GP), which displayed the most significant differences, $p < 0.0001$, in both viscosity and viscoelasticity. Hydrogel H1 (2.5% w/v GP) exhibited the lowest gelation temperature and the fastest gelation time (19.6 ± 0.6 °C, 13 ± 4 s), since the long polymer chains formed extensive hydrophobic interactions. Formulation H2 (5% w/v GP) did not show significant thermoresponsive behaviour with respect to the apparent viscosity (Fig. 4b); the higher degree of quaternisation increased solubility and enhanced electrical repulsion between TMC chains to prevent a substantial change in viscosity. These data are in agreement with the literature, demonstrating that the components concentration and polymer characteristics all have an effect over the gelation time and temperature of the formulation [42–44].

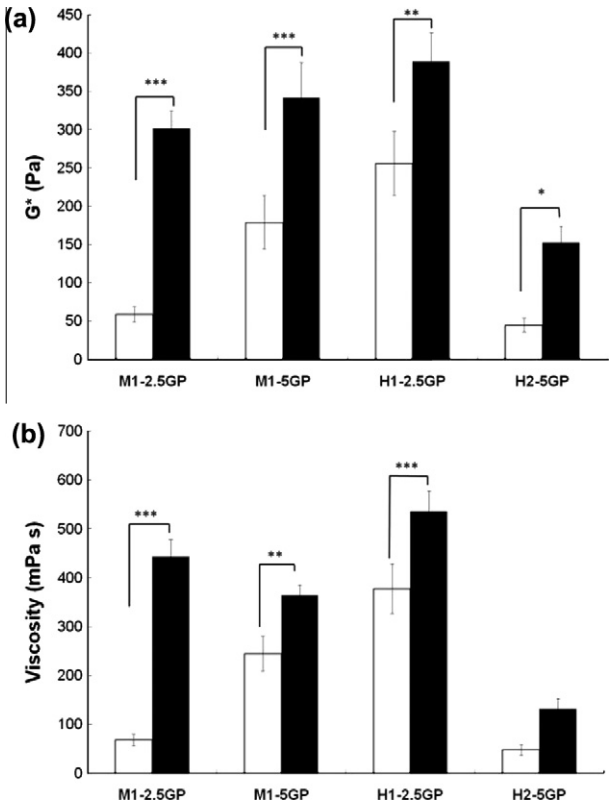

Fig. 4. (a) Complex modulus (G^*) and (b) apparent viscosity values for TMC hydrogel formulations at 15 °C (white) and at 35 °C (black). Results are given as mean ± SD ($n = 4$): $^{***}p < 0.001$, $^{**}p < 0.01$, $^{*}p < 0.05$; Tukey–Kramer post hoc comparison test.

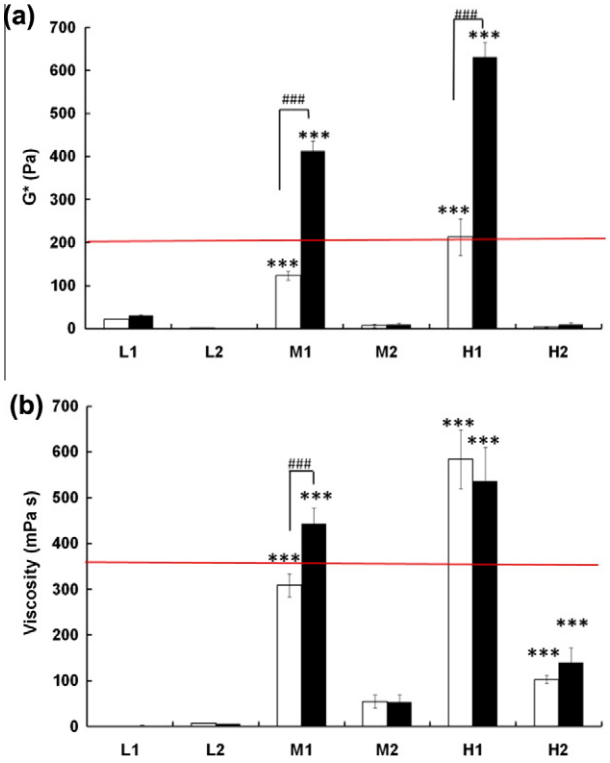

Fig. 5. (a) Complex modulus (G^*) and (b) apparent viscosity at 15 °C (white) and 35 °C (black) of hydrogel–mucin mixtures. All formulations were prepared with 2.5% GP. Values are given as mean ± SD ($n = 4$). Data above the red line indicate (a) G^* values required to decrease MTR by at least 80% and (b) η values required to decrease MTR by at least 60% [30]: $^{###}p < 0.001$, comparing 15–35 °C, $^{***}p < 0.001$ with respect to water; Tukey–Kramer post hoc comparison test. (For interpretation of the references to colour in this figure legend, the reader is referred to the web version of this article.)

3.2.2. Rheological properties of the hydrogels

Fig. 5 summarises G^* and η data – the rheological properties of polymer–mucus mixtures that have a most significant impact on MTR [30] – for hydrogel–mucin mixtures at 15 and at 35 °C. The very significant ($p < 0.001$) increase in G^* seen for M1 and for H1 is consistent with mixtures that are capable of exhibiting prolonged residence in the nasal cavity [30]. The complex modulus (G^*), which describes the rigidity and overall strength of the gel, is used as a parameter to monitor the effect on MTR. Gels of increasing G^* were found to increasingly reduce MTR, due to the inability of the cilia to penetrate effectively into the gel (elastic properties), decreasing the efficiency of energy transfer to the mucus/polymer layer (viscous properties) [30]. At 35 °C, the same hydrogel–mucin mixtures displayed apparent viscosity values >350 mPa s, but at 15 °C only M1 mixtures had viscosities <350 mPa s, identifying M1 as the material of choice for the formulation of thermosensitive nasal sprays or drops. Hydrogels L1 and L2 appeared to be of little value to nasal delivery since their rheological properties were not significantly different to those of water ($p > 0.05$) at either temperature. Similarly, hydrogels M2 and H2 did not meet the requirements ($G^* > 200$ Pa; $\eta > 350$ mPa s) for use as thermosensitive nasal-delivery systems [30].

3.2.3. Hydrogels–mucin interactions

Oscillation profiles of L1, M1 and H1 and of their mixtures with mucin are presented in Fig. 6, along with those of mucin alone. The storage and loss *moduli* of mucin show some frequency dependency, with a crossover at *ca.* 2 Hz, as is typical of the behaviour of weakly entangled polymeric systems [45]. The observed behaviour

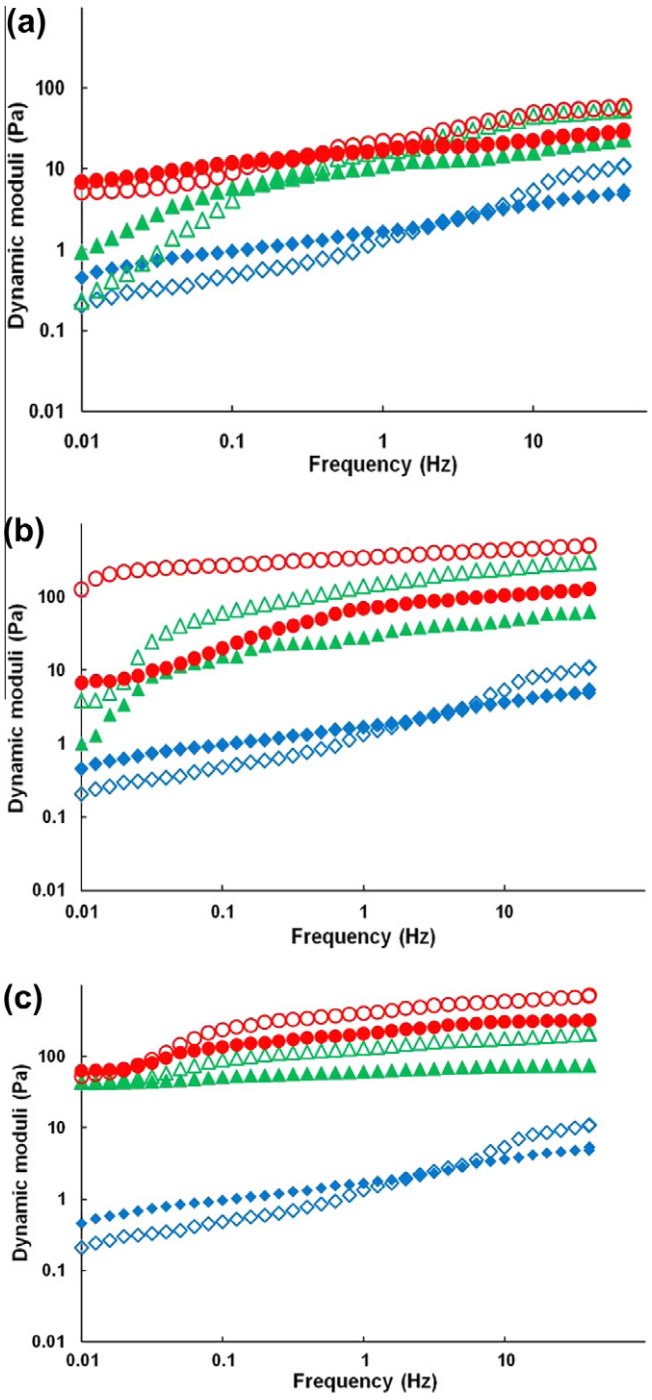

Fig. 6. Dynamic oscillation spectra of TMC hydrogels and of their mixtures with mucin: (a) L1; (b) M1; and (c) H1 – G' hydrogel–mucin (⬭); G'' hydrogel–mucin (●); G' hydrogel (△); G'' hydrogel (▲); G' mucin (◇), G'' mucin (◆). (For interpretation of the references to colour in this figure legend, the reader is referred to the web version of this article.)

of mucin is different to that of physiological mucus, for which $G' > G''$ over the entire frequency range [46]. The oscillation spectra of M1–mucin mixtures (Fig. 6b) show that $G' > G''$ over the entire frequency range, which is consistent with the behaviour of a strongly cross-linked gel [46], consequently indicating that there is substantial interaction between the hydrogel and the mucin. By contrast, L1–mucin mixtures (Fig. 6a) behave as a physically entangled system, exhibiting $G'' > G'$ over a broad spectral range along with a substantial decline in G', and to a lesser extent G'', at low frequencies [46], therefore showing a lower degree of interaction between the two systems upon mixing. The oscillation spectra of the H1–mucin mixture, Fig. 6c, show a predominance of elastic behaviour ($G' > G''$) with some degree of physical entanglement ($G'' > G'$) at lower frequencies. The mixing of H1 with mucin results in a more pronounced increase in G'' than in G', which is interpreted as an increase in the fluidity of the system, since there is a low degree of entanglement between the longer coiled TMC chains and mucin, decreasing mucoadhesive potential. Comparison of the rheology profiles of L2, M2 and H2 with those of their mixtures with mucin reveals no significant differences in dynamic *moduli*. For these materials, the increase in aqueous solubility following the quaternisation of TMC is accompanied by a predominance of viscous properties and a suppression of the elasticity of the hydrogel. Since all materials share the chemical features of chitosan, their capacity to enter into rheologically synergistic relationship with mucin must be a direct consequence of the combined effects of their average molecular weight and degree of quaternisation [17,47–49].

The addition of mucin to the H1 hydrogel, Fig. 7, effects an increase in G', indicative of the homogeneity of the mixture, and a more pronounced increase in G'', which shows that mucin/H1 mixtures are less elastic and more viscous than the parent hydrogel. The relative G' of the mucin/M1 mix, Fig. 7, is consistent with the high compatibility of the constituent materials in their forming of homogeneous mixtures.

3.3. Mucoadhesive behaviour

As is prerequisite to good mucoadhesive behaviour, all hydrogels displayed their capacity to hydrate readily and hold high quantities of water (Fig. 8a) [49–54]. The water-holding capacities of the low degree of quaternisation hydrogels M1 and H1 are comparable with those of poly(acrylic acid), the archetypal mucoadhesive polymer. Complementary work-of-adhesion measurements identify M1 as the hydrogel of choice for employment in mucoadhesive formulations: M1 is the only material that yielded work-of-adhesion values (252 ± 14 μJ) that are comparable with those of poly(acrylic acid) ($p > 0.05$). The work-of-adhesion values determined for hydrogels L1, L2, M2 and H2 were similar ($p > 0.05$) to that obtained for tristearin, the negative control (Fig. 8b). The results correlate with those from rheological investigations and highlight the complementarity of the techniques in the evaluation of the mucoadhesive potential of a material.

3.4. Physicochemical characterisation of hydrogels

As is exemplified by infrared spectroscopy of M1 (see ESI), hydrogels exhibit the vibrational features of all constituents of

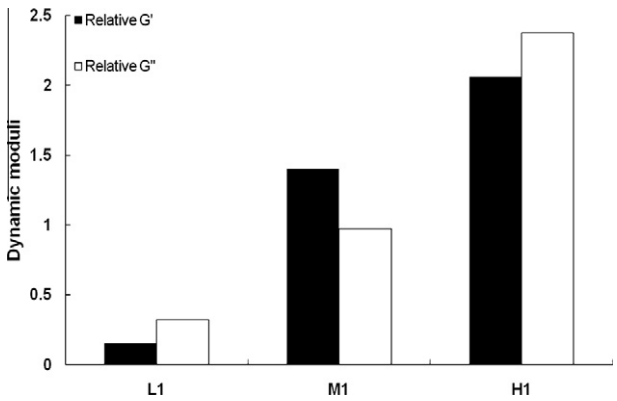

Fig. 7. The synergistic effect of TMC hydrogels–mucin mixtures evaluated using relative G' and G'' values at 35 °C.

the formulation: features associated with PEG are evident at the aliphatic C–H stretch region (*ca.* 2700 cm^{-1}) and also in the skeletal fingerprint region, whereas TMC manifests itself in the hydrogen-bonded region (>3000 cm^{-1}). In M1, the broad absorption arising from hydrogen-bonded interactions due to the –NH and –OH functionalities of the TMC constituent of the hydrogel is shifted to higher frequencies relative to those of pure TMC. This shift is consistent with the predominance of intermolecular hydrogen bonding over corresponding intra-molecular interactions [55] and confirms the homogeneous nature of the formulation.

Surface area analysis, Fig. 9, shows that in a direct relationship with the average molecular weight of each material, S_{BET} (Fig. 9b) adopts values that are as low as 0.08 $m^2 g^{-1}$ or as high as 4.88 $m^2 g^{-1}$. This trend corresponds with SEM images of pore size, Fig. 9 a, and with determinations of pore volume, Fig. 9c: hydrogels that had been dried for SEM imaging exhibited pore diameters varying from *ca.* 4 nm to 1 μm. As expected [56], trends in porosity and S_{BET} data follow those for water-holding capacity; hydrogels that hold more water present higher porosity values. With the exception of H1, the mucoadhesive behaviour of the materials also correlated well with trends in internal surface area and porosity. Furthermore, porosity data can help predict the diffusion of drug molecules within the gel [15,57,58].

4. Conclusion

Co-formulation of poly(ethylene glycol) and glycerophosphate with *N*-trimethyl chitosan of medium average molecular weight and low degree of quaternisation yields an aqueous formulation that exhibits a sol–gel transition at 32.5 °C and within 7 min. The same hydrogel forms rheologically synergistic mixtures with mucus and also exhibits good affinity for mucosal surfaces. The properties of this hydrogel appear to be consistent with its potential use as an *in situ* thermogelling drug–carrier system for intranasal drug delivery. Further studies are underway to investigate its absorption enhancing properties and biocompatibility. Positive preliminary results indicate this is a promising formulation.

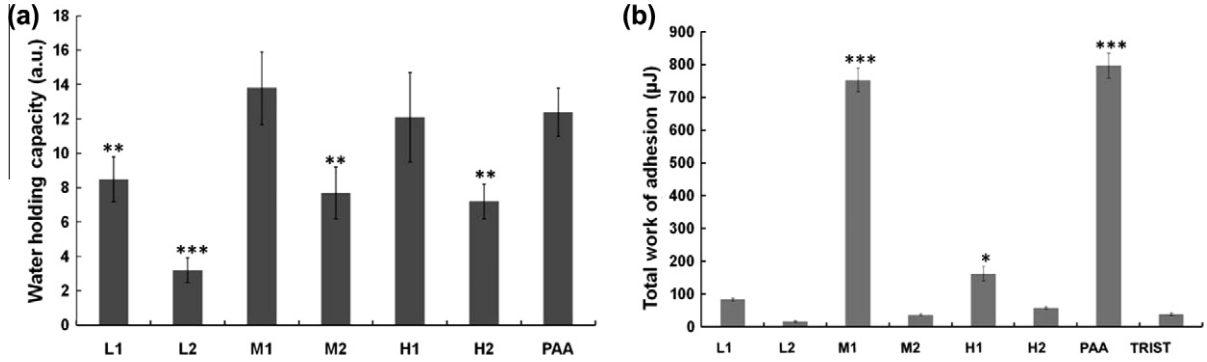

Fig. 8. (a) Water-holding capacity (WHC; mean ± SD, $n = 5$) of hydrogel formulations in SNES-mucin solutions: $^{**}p < 0.001$, $^{***}p < 0.0001$ with reference to M1; Tukey–Kramer post hoc comparison test. (b) Total work-of-adhesion (TWA; mean ± SD, $n = 5$) of TMC hydrogels, poly(acrylic acid) (positive control) and tristearin (negative control): $^{***}p < 0.001$ and $^{*}p < 0.05$ with respect to the positive control; Tukey–Kramer post hoc comparison test.

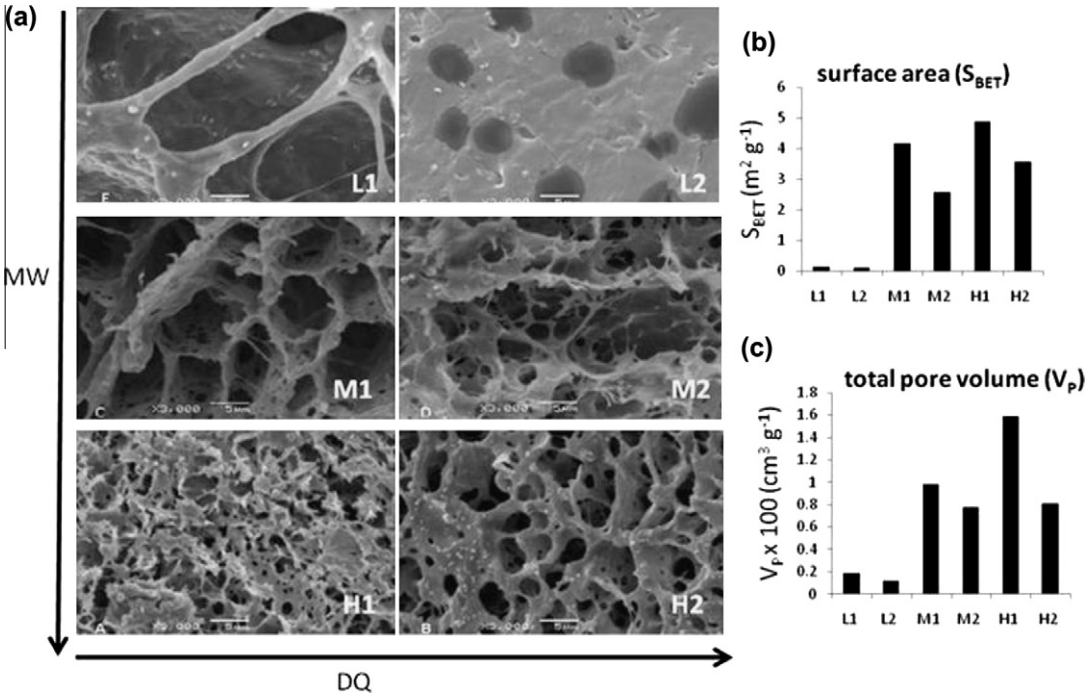

Fig. 9. (a) SEM micrographs, (b) surface area (S_{BET}), and (c) total pore volume (V_P) of hydrogel formulations.

Appendix A. Supplementary material

Supplementary data associated with this article can be found, in the online version, at doi:10.1016/j.ejpb.2010.11.022.

References

[1] M.I. Ugwoke, R.U. Agu, N. Verbeke, R. Kinget, Nasal mucoadhesive drug delivery: background, applications, trends and future perspectives, Adv. Drug Deliv. Rev. 57 (2005) 1640–1665.
[2] R.U. Agu, H.V. Dang, M. Jorissen, T. Willems, R. Kinget, N. Verbeke, Nasal absorption enhancement strategies for therapeutic peptides: an in vitro study using cultured human nasal epithelium, Int. J. Pharm. 237 (2002) 179–191.
[3] M. Amidi, S.G. Romeijn, G. Borchard, H.E. Junginger, W.E. Hennink, W. Jiskoot, Preparation and characterization of protein-loaded *N*-trimethyl chitosan nanoparticles as nasal delivery system, J. Control. Release 111 (2006) 107–116.
[4] E.S. Khafagy, M. Morishita, K. Isowa, J. Imai, K. Takayama, Effect of cell-penetrating peptides on the nasal absorption of insulin, J. Control. Release 133 (2009) 103–108.
[5] T. Kissel, U. Werner, Nasal delivery of peptides: an in vitro cell culture model for the investigation of transport and metabolism in human nasal epithelium, J. Control. Release 53 (1998) 195–203.
[6] J. Wang, Y. Tabata, K. Morimoto, Aminated gelatin microspheres as a nasal delivery system for peptide drugs: evaluation of in vitro release and in vivo insulin absorption in rats, J. Control. Release 113 (2006) 31–37.
[7] M.I. Ugwoke, N. Verbeke, R. Kinget, The biopharmaceutical aspects of nasal mucoadhesive drug delivery, J. Pharm. Pharmacol. 53 (2001) 3–21.
[8] A. Pires, A. Fortuna, G. Alves, A. Falcao, Intranasal drug delivery: how, why and what for?, J Pharm. Pharmaceut. Sci. 12 (2009) 288–311.
[9] N. Uchida, Y. Maitani, Y. Machida, M. Nakagaki, T. Nagai, Influence of bile-salts on the permeability of insulin through the nasal-mucus of rabbits in comparison with dextran derivatives, Int. J. Pharm. 74 (1991) 95–103.
[10] N.M. Zaki, G.A. Awad, N.D. Mortada, S.S. Abd ElHady, Enhanced bioavailability of metoclopramide HCl by intranasal administration of a mucoadhesive in situ gel with modulated rheological and mucociliary transport properties, Eur. J. Pharm. Sci. 32 (2007) 296–307.
[11] D. Elad, M. Wolf, T. Keck, Air-conditioning in the human nasal cavity, Respir. Physiol. Neurobiol. 163 (2008) 121–127.
[12] N. Mygind, R. Dahl, Anatomy, physiology and function of the nasal cavities in health and disease, Adv. Drug Deliv. Rev. 29 (1998) 3–12.
[13] L. Mayo, F. Quaglia, A. Borzacchiello, L. Ambrosio, M.I. La Rotonda, A novel poloxamers/hyaluronic acid in situ forming hydrogel for drug delivery: rheological, mucoadhesive and in vitro release properties, Eur. J. Pharm. Biopharm. 70 (2008) 199–206.
[14] J. Wu, W. Wei, L.-Y. Wang, Z.-G. Su, G.-H. Ma, A thermosensitive hydrogel based on quaternized chitosan and poly(ethylene glycol) for nasal drug delivery system, Biomaterials 28 (2007) 2220–2232.
[15] G.P. Andrews, T.P. Laverty, D.S. Jones, Mucoadhesive polymeric platforms for controlled drug delivery, Eur. J. Pharm. Biopharm. 71 (2009) 505–518.
[16] J.W. Lee, J.H. Park, J.R. Robinson, Bioadhesive-based dosage forms: the next generation, J. Pharm. Sci. 89 (2000) 850–866.
[17] F. Madsen, K. Eberth, J.D. Smart, A rheological examination of the mucoadhesive/mucus interaction: the effect of mucoadhesive type and concentration, J. Control. Release 50 (1998) 167–178.
[18] J. Berger, A. Reist, A. Chenite, O. Felt-Baeyens, J.M. Mayer, R. Gurny, Pseudo-thermosetting chitosan hydrogels for biomedical application, Int. J. Pharm. 288 (2005) 197–206.
[19] H.Q. Chen, M.W. Fan, Novel thermally sensitive pH-dependent chitosan/carboxymethyl cellulose hydrogels, J. Bioactive Compatible Polym. 23 (2008) 38–48.
[20] M.N.V.R. Kumar, R.A.A. Muzzarelli, C. Muzzarelli, H. Sashiwa, A.J. Domb, Chitosan chemistry and pharmaceutical perspectives, Chem. Rev. 104 (2004) 6017–6084.
[21] L.S. Nair, T. Starnes, J.W.K. Ko, C.T. Laurencin, Development of injectable thermogelling chitosan-inorganic phosphate solutions for biomedical applications, Biomacromolecules 8 (2007) 3779–3785.
[22] S.M. van der Merwe, J.C. Verhoef, J.H.M. Verheijden, A.F. Kotzé, H.E. Junginger, Trimethylated chitosan as polymeric absorption enhancer for improved peroral delivery of peptide drugs, Eur. J. Pharm. Biopharm. 58 (2004) 225–235.
[23] A. Chenite, M. Buschmann, D. Wang, C. Chaput, N. Kandani, Rheological characterisation of thermogelling chitosan/glycerol-phosphate solutions, Carbohydr. Polym. 46 (2001) 39–47.
[24] A.F. Kotze, H.L. Luessen, B.J. deLeeuw, B.G. deBoer, J.C. Verhoef, H.E. Junginger, *N*-trimethyl chitosan chloride as a potential absorption enhancer across mucosal surfaces: In vitro evaluation in intestinal epithelial cells (Caco-2), Pharm. Res. 14 (1997) 1197–1202.
[25] Y. Chang, L. Xiao, Y. Du, Preparation and properties of a novel thermosensitive *N*-trimethyl chitosan hydrogel, Polym. Bull. 63 (2009) 531–545.
[26] A.B. Sieval, M. Thanou, A.F. Kotze, J.E. Verhoef, J. Brussee, H.E. Junginger, Preparation and NMR characterization of highly substituted *N*-trimethyl chitosan chloride, Carbohydr. Polym. 36 (1998) 157–165.
[27] F. Chen, Z.R. Zhang, Y. Huang, Evaluation and modification of *N*-trimethyl chitosan chloride nanoparticles as protein carriers, Int. J. Pharm. 336 (2007) 166–173.
[28] J. Wu, Z.G. Su, G.H. Ma, A thermo- and pH-sensitive hydrogel composed of quaternized chitosan/glycerophosphate, Int. J. Pharm. 315 (2006) 1–11.
[29] Q.X. Ji, Q.S. Zhao, J. Deng, R. Lu, A novel injectable chlorhexidine thermosensitive hydrogel for periodontal application: preparation, antibacterial activity and toxicity evaluation, J. Mater. Sci. – Mater. Med. 21 (2010) 2435–2442.
[30] A. Shah, M. Donovan, Formulating gels for decreased mucociliary transport using rheological properties: polyacrylic acids, AAPS Pharm. Sci. Technol. 8 (2007) (article 33).
[31] J.H. Hamman, A.F. Kotze, Effect of the type of base and number of reaction steps on the degree of quaternization and molecular weight of *N*-trimethyl chitosan chloride, Drug Dev. Ind. Pharm. 27 (2001) 373–380.
[32] M. Thanou, A.F. Kotze, T. Scharringhausen, H.L. Luessen, A.G. de Boer, J.C. Verhoef, H.E. Junginger, Effect of degree of quaternization of *N*-trimethyl chitosan chloride for enhanced transport of hydrophilic compounds across intestinal Caco-2 cell monolayers, J. Control. Release 64 (2000) 15–25.
[33] H. Chung, H. Dong, Synthesis and characterisation of pluronic grafted chitosan copolymer as a novel injectable biomaterial, Curr. Appl. Phys. 5 (2005) 485–488.
[34] R.G. Riley, J.D. Smart, J. Tsibouklis, P.W. Dettmar, F. Hampson, J.A. Davis, G. Kelly, W.R. Wilber, An investigation of mucus/polymer theological synergism using synthesised and characterised poly(acrylic acid)s, Int. J. Pharmaceut. 217 (2001) 87–100.
[35] I.K. Han, Y.B. Kim, H.S. Kang, D. Sul, W.W. Jung, H.J. Cho, Y.K. Oh, Thermosensitive and mucoadhesive delivery systems of mucosal vaccines, Methods 38 (2006) 106–111.
[36] M. Hasegawa, A. Isogai, F. Onabe, M. Usuda, R.H. Atalla, Characterization of cellulose chitosan blend films, J. Appl. Polym. Sci. 45 (1992) 1873–1879.
[37] C.E. Orrego, N. Salgado, J.S. Valencia, G.I. Giraldo, O.H. Giraldo, C.A. Cardona, Novel chitosan membranes as support for lipases immobilization: characterization aspects, Carbohydr. Polym. 79 (2010) 9–16.
[38] W. Groenewoud, Characterisation of Polymers by Thermal Analysis, first ed., Elsevier Science, Amsterdam, 2001.
[39] S. Kumar, J. Dutta, P.K. Dutta, Preparation and characterization of *N*-heterocyclic chitosan derivative based gels for biomedical applications, Int. J. Biol. Macromol. 45 (2009) 330–337.
[40] S. Green, M. Roldo, D. Douroumis, N. Bouropoulos, D. Lamprou, D.G. Fatouros, Chitosan derivatives alter release profiles of model compounds from calcium phosphate implants, Carbohydr. Res. 344 (2009) 901–907.
[41] R.J. Soane, M. Frier, A.C. Perkins, N.S. Jones, S.S. Davis, L. Illum, Evaluation of the clearance characteristics of bioadhesive systems in humans, Int. J. Pharm. 178 (1999) 55–65.
[42] F. Ganji, M.J. Abdekhodaie, A. Ramanzi, Gelation time and degradation rate of chitosan-based injectable hydrogel, J. Sol–Gel Sci. Technol. 42 (2007) 47–53.
[43] Q.X. Ji, J. Deng, X.M. Xing, C.Q. Yuan, X.B. Yu, Q.C. Xu, J. Yue, Biocompatibility of chitosan-based injectable thermosensitive hydrogel and its effects on dog periodontal tissue regeneration, Carbohydr. Polym. 82 (2010) 1153–1160.
[44] S. Kim, S.K. Nishimoto, J.D. Bumgardner, W.O. Haggard, M.W. Gaber, Y. Yang, A chitosan/β-glycerophosphate thermo-sensitive gel for the delivery of ellagic acid for the treatment of brain cancer, Biomaterials 31 (2010) 4157–4166.
[45] P. Sriamornsak, N. Wattanakorn, Rheological synergy in aqueous mixtures of pectin and mucin, Carbohydr. Polym. 74 (2008).
[46] F. Madsen, K. Eberth, J.D. Smart, A rheological assessment of the nature of interactions between mucoadhesive polymers and a homogenised mucus gel, Biomaterials 19 (1998) 1083–1092.
[47] S.A. Mortazavi, B.G. Carpenter, J.D. Smart, An investigation of the rheological behavior of the mucoadhesive mucosal interface, Int. J. Pharm. 83 (1992) 221–225.
[48] S.A. Mortazavi, B.G. Carpenter, J.D. Smart, A comparative-study on the role played by mucus glycoproteins in the rheological behavior of the mucoadhesive mucosal interface, Int. J. Pharm. 94 (1993) 195–201.
[49] S.A. Mortazavi, J.D. Smart, Factors influencing gel-strengthening at the mucoadhesive–musuc interface, J. Pharm. Pharmacol. 46 (1994) 86–90.
[50] C.B. He, F.Y. Cui, L.C. Yin, F. Qian, C. Tang, C.H. Yin, A polymeric composite carrier for oral delivery of peptide drugs: bilaminated hydrogel film loaded with nanoparticles, Eur. Polym. J. 45 (2009) 368–376.
[51] Q.Z. Li, D.Z. Yang, G.P. Ma, Q. Xu, X.M. Chen, F.M. Lu, J. Nie, Synthesis and characterization of chitosan-based hydrogels, Int. J. Biol. Macromol. 44 (2009) 121–127.
[52] M. Roldo, M. Hornof, P. Caliceti, A. Bernkop-Schnurch, Mucoadhesive thiolated chitosans as platforms for oral controlled drug delivery: synthesis and in vitro evaluation, Eur. J. Pharm. Biopharm. 57 (2004) 115–121.
[53] A. Jintapattanakit, S. Mao, T. Kissel, V.B. Junyaprasert, Physicochemical properties and biocompatibility of *N*-trimethyl chitosan: effect of quaternization and dimethylation, Eur. J. Pharm. Biopharm. 70 (2008) 563–571.
[54] D. Snyman, J.H. Hamman, A.F. Kotze, Evaluation of the mucoadhesive properties of *N*-trimethyl chitosan chloride, Drug Dev. Ind. Pharm. 29 (2003) 61–69.
[55] L.M. Harwood, T.D.W. Claridge, Introduction to Organic Spectroscopy, Oxford University Press, Great Britain, 1996.
[56] B.B. Mandal, S. Kapoor, S.C. Kundu, Silk fibroin/polyacrylamide semi-interpenetrating network hydrogels for controlled drug release, Biomaterials 30 (2009) 2826–2836.
[57] N. Bhattarai, J. Gunn, M. Zhang, Chitosan-based hydrogels for controlled, localized drug delivery, Adv. Drug Deliv. Rev. 62 (2010) 83–99.
[58] C.-C. Lin, A.T. Metters, Hydrogels in controlled release formulations: network design and mathematical modeling, Adv. Drug Deliv. Rev. 58 (2006) 1379–1408.